

Integration of Sorption Collector in Office Curtain Wall: Simulation Based Comparison of Different System Configurations

Stefano Avesani¹, Olof Hallström², Gerrit Földner³ and Roberto Fedrizzi¹

¹ Institute for Renewable Energy – Eurac Research, Bolzano (Italy)

² Mälardalen University, Västerås (Sweden)

³ Fraunhofer Institute für Solar Energiesysteme, Freiburg (Germany)

Abstract

European trends push towards the smart integration of renewables in building components guaranteeing robust and plug & play solutions. This approach seems particularly favorable for the retrofit sector, where, nevertheless, there is still a big lack of this kind of products. In this direction, a solar cooling “double integrated” system has been designed and assessed. A solution has been developed to directly integrate a triple state absorption module - with LiCl and water as working couple - in a Sydney type vacuum tube solar collector (Hallström et al. 2014). Secondly, a system layout for integrating this component in a metal-glass curtain wall has been defined. The result is a fully integrated solar active façade module directly generating and distributing heating and cooling to the indoor environment. Sorption collectors with air-based heat transfer have been modeled and simulated in order to depict components and overall system performance figures needed for the prototype integration in the building system. A TRNSYS model, based on validated components, has been parametrically run and simulation results analyzed. Results highlight a quantitative and qualitative analysis of potentials and limits of this double integrated (façade and solar collector) cooling technology.

Key-words: solar cooling, building integration, sorption collector.

1. Introduction

As described in (Hallström, et al. 2014), the patented triple state absorption module - with LiCl and water as working couple- is based on a batch process similar to adsorption and occurs in a sealed glass tube under vacuum. Besides the absorption module, one major innovation comes from the way this technology is integrated into a complete solar cooling system. By linking the heat source (sun power through the collector absorber) directly with the sorption material, the system is greatly simplified. Instead of pumping hot water from a solar collector, the sorption units are integrated into the solar collector and hence heated directly by the solar irradiation. Each sorption unit can be conceptually divided in two parts: the reactor and the condenser/evaporator. A variable number of units are then connected by one heat exchanger at the reactor and one other at the condenser/evaporator sides. Since solar irradiation is only available during the day, day time is naturally reserved for desorption: salt solution desorbs in the reactor with simultaneous heat rejection at the condenser; when irradiation stops, absorption can run with cooling effect at the evaporator and heat rejection at the reactor. Hence, de- and absorption times are depending on the presence of direct solar radiation and therefore on the façade orientation.

The concept has already been proven for an integrated flat plate sorption collector for roof installations in the EU LIFE11 ENV/SE/838 SUNCOOL project as reported in (Blackman, et al., 2014) and (Hallström, et al., 2014). The dynamic interaction with the building energy system as a whole and further developments of the prototype aim at decreasing system complexity, lowering costs and increasing performance. Hence, these activities have been taken over within EU FP7 Inspire project (www.fp7inspire.eu) in order to integrate sorption modules in a vacuum tube collector and the overall component in the opaque part of a standard metal-glass façade module. Two main layout concepts have been developed for the façade integrated collector, one

using liquid (water or water/glycol) and one air as heat transfer medium. Similar for both concepts are the thermal processes within the tubes and the main operation cycles. On the contrary, main differences between the two concepts are in how the energy is transferred from the sorption modules to the heat transfer medium and to the indoor air and how the collector interacts with the building heating and cooling system. Air-based concept seems to be more promising because of the following reasons among others. Firstly, the overall aeraulic system is less complex than a hydraulic layout - for example, there is no need for a dry cooler for heat rejection or for a water-water heat exchanger for power distribution to the indoor ambient. Then, all components are independent from the other building services: it needs just electric power connection and no valves for the coupling to the existing energy system. Finally, the design of the internal heat exchangers is simpler. A graphic layout of the air based sorption collector is illustrated in Fig. 1.

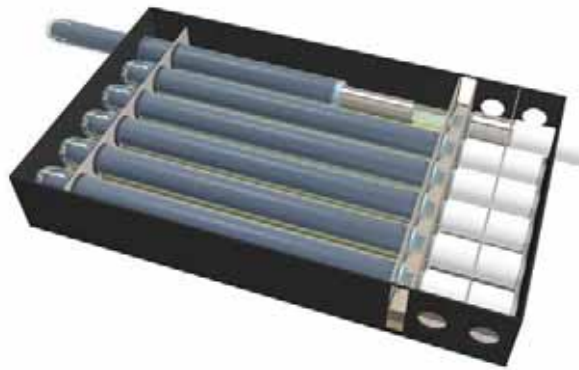


Fig. 1: Graphic layout of the complete air-based sorption collector

Cellular metal-glass curtain walls for the retrofit of existing building are an interesting field of application of the sorption collector technology. Firstly, this façade typology is mainly prefabricated offering good possibility of integration of other components directly in the production line. Hence, the façade integrated sorption solar collector can offer a “plug and play” and turnkey solution. Secondly, in the field of retrofit, old curtain walls can be removed and replaced with new ones with relative simplicity. Furthermore, cooling and electric loads are usually relevant also in cold climate. Finally, in tertiary office buildings’ the degree of penetration of sustainable retrofit seems to be higher (Itard, et al., 2008).

The work here presented investigates the energy performance of a façade integrated air-based sorption collector for the retrofit of existing office buildings. It provides performance data for the system integrated with a building room showing the directions for further developments and analyses to be done as next steps.

2. Methods

2.1 Air-based sorption collector description

The air-based sorption collector operation principles are the same as for the water-based system and are well explained in (Hallström, et al. 2014) and (Földner, et al., 2013). A first air-based prototype has been developed and built in order to verify its performances. It is composed by four sorption tubes, each one integrated in a custom made evacuated Sydney type vacuum tube and wrapped in a folded aluminium sheet heat exchanger on both the reactor and condenser/evaporator side. The reflectors have been specifically designed for this application in order to maximise the optical efficiency of the collector.

The prototype has been tested in lab under controlled boundary conditions and its operation verified and characterised from an energy and fluid dynamic point of view. Some of the results from the measurements are shown in Fig. 2. The test results have been used to verify the design assumptions made and to calibrate a dynamic TRNSYS model which is similar to the one described in Hallström, et al. 2014.

To be competitive from a design point of view, the façade integrated sorption collector has to be composed by the easiest configuration of electric, aeraulic and hydraulic components in order to reduce the electric parasitic consumption, the installation and maintenance efforts. A possible aeraulic layout is shown in Fig. 3. The system is based on standard aeraulic components: two constant speed fans and eight controlled dampers. This configuration allows all possible heat exchanges among reactor, condenser/evaporator, indoor and outdoor environments. Hence, for example, heat rejection could be realized using either indoor or outdoor air depending

on the available temperatures and season.

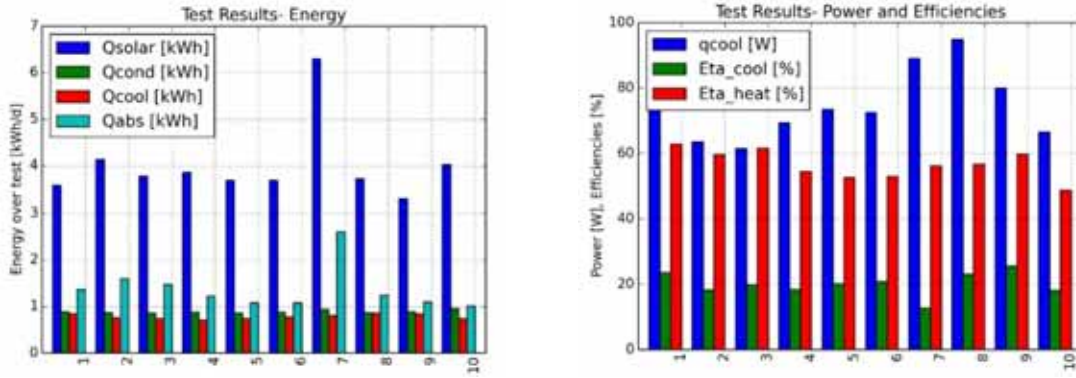


Fig. 2: Energies, powers and heating and cooling efficiency for the 10 dynamic test measurements.

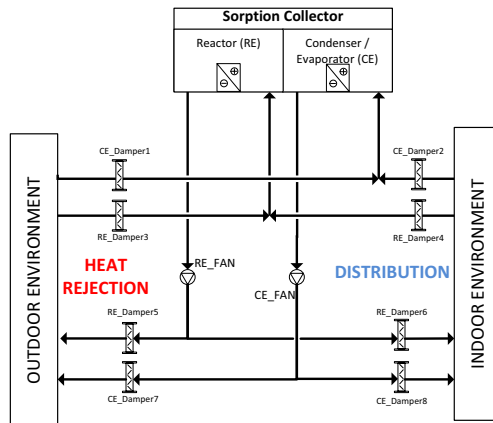


Fig. 3: Conceptual sketch of the air-based sorption collector aeraulic layout

2.2 Reference façade and room

The sorption collector has been then further developed for its integration in a curtain wall serving an office building. The curtain wall considered is a cellular metal-glass double skin façade module (1.5 m width and 3 m height) with opaque parts below and above the transparent one. The glazed part is composed by an internal double glazing, about 0.2 m of air cavity and an external single glazing. The upper part of the cavity hosts a small fan for the façade ventilation and for the retractable shading system (standard venetian blinds). The reference curtain wall has a transparent to total areas ratio of about 2/3, following the most common architectural trends of office building. The sorption collector is integrated in the lower opaque area, in a depth of circa 0.3 m with a 8 mm single glazing covering frontally the collector for safety reasons and giving the façade the one single plane appearance. The upper opaque part cannot be exploited as active surface in the current version of the façade module and therefore it has been considered neither for the sorption collector nor for the building physic calculation. Hence, the façade module can be simplified as in Fig. 4.

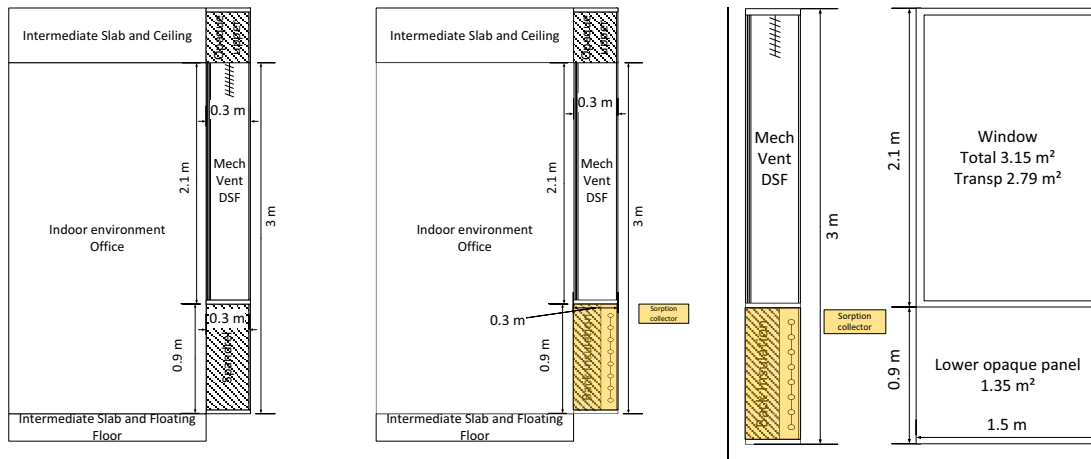


Fig. 4: Simplified sketches of the façade and of the sorption collector integration

The aeraulic layout proposed in the previous paragraph has still to be designed in detail and therefore is not represented in Fig. 4.

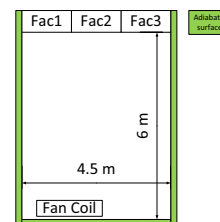
An office of 6 m depth and 4.5 m wide with three workers has been considered as reference room. It is equipped with one fancoil acting as backup, connected with the building energy system. Moreover, the room has a primary ventilation system assuring the needed hygienic air changes.

2.3 Façade integrated sorption collector model description

The overall system model has been done in TRNSYS 17, joining together different sub-models following the real components layout. Type 56 is used as building model. At the current step of the study, the mechanically ventilated double skin façade has been simplified to a single skin that is also only non-adiabatic surface. This simplification is realistic considering a general office room at an intermediate floor of a tertiary building: the more floors the building have, the closer thermal behavior to the model the room will show. The façade construction follows the specification of standard curtain walls: double glazing system (U-value of 1.1 W/m²K and g-value of 0.5), external movable shading ($\tau = 0.15$, $\alpha = 0.35$, $\rho = 0.5$) and highly insulated spandrel with external opaque glazing (U-value of about 0.3 W/m²K). The other main building model boundary conditions are summarized in Tab. 1 and Tab. 2.

Tab. 1: Summary of the main room geometry boundary conditions

Parameter	Unit of measure	Value
Office area	[m ²]	27
Office air volume	[m ³]	81
Nr of façade module	[mod]	3
Nr of adiabatic surfaces	[nr surf]	5



Internal brick walls, floating floor and suspended ceiling are set in the model. More detailed information about the room simulation boundary conditions are provided in (Di Pasquale et al., 2014).

Tab. 2: Room model boundary conditions

Parameter	Unit of measure	Value
Nr workers	[worker]	3
Fresh air changes per person	[m ³ /s/p]	0.011
External air infiltration	[1/h]	0.15
Appliances electric load	[W/m ²]	16
Lighting electric load	[W/m ²]	12.5
Heating set point (hysteresis)	[°C]	21 (-1)
Cooling set point (hysteresis)	[°C]	25 (+1)

The building model is intended to be enough general to represent a common office room. It has not been validated against measured values, even if cooling and heating energy demands are in line with the results in (Di Pasquale, et al., 2014).

The sorption collector is modelled with type 827 (Hallström, et al. 2014) for the sorption tube and type 832 (Haller, 2012) for the optical transmission of solar irradiation. Type 827 gives as output the whole set of collector temperatures and powers. These values are needed to couple the sorption collector and the building model. The room spandrel is dynamically coupled to the sorption collector back temperature. On the contrary, the influence of the indoor air temperature on the sorption collector performance has not been modeled under the reasonable assumption of low heat fluxes due to the thick insulation layer on the collector back. The façade integrated sorption collector has an aperture area (coincident with the reactor side of the collector) of 0.89 m² per façade module. External glazed cover, Sydney tubes and reflectors optical performances have been

calculated using ray tracing method during the design phase providing the longitudinal and transversal IAM for the façade integrated sorption collector configuration.

Fans, dampers and ducts of the aeraulic layout are simulated with standard component from the TRNSYS (base and TESS) libraries. Hygrometric air properties at the collector inlet and outlet are calculated. Fans power has been calculated starting from the hypotheses of a constant fan electric efficiency of 13%. This value has been derived from the datasheet of a commercial axial fan. From the efficiency, the actual consumption for different pressure drops and mass flow rates can be calculated as $q_{el} = eff \cdot q_{mech}$ (eq. 1). The pressure drop-mass flow rate curve was available thanks to the lab measurements. In order to achieve a good difference of temperature, mass flow rate is set to 30 kg/h/m²ap. Hence, the calculated electric power consumption are 1.74 W/m²ap and 4.86 W/m²ap respectively for the RE and CE fans.

Weather data used in simulations are taken from Meteonorm, with statistical data for the period 1986-2005 for global radiation and 2000-2009 for temperature, humidity, precipitation and wind speed.

The main model limitation are therefore: mechanically ventilated DSF is simplified into a single skin with double glass and external shading system; the thermal influence of the room indoor air on the sorption collector behavior is neglected; the air hygrometric properties are calculated, but the condenser outlet air temperature is not adjusted in case of condensation meaning that the sorption collector act only on the sensible heat transfer.

2.4 Sorption collector model calibration

The testing of the prototype collector has been performed in a solar simulator at the Fraunhofer Institute Solar Energy Systems (ISE) in Freiburg. The collector was set up perpendicular to the solar lamps and connected to air inlet and outlet on both reactor and condenser/evaporator side. Four different types of steady state measurements have been used to calculate the optical efficiency as well as all thermal loss coefficient of the model, i.e. reactor tube losses, reactor manifold losses, C/E manifold losses, and internal losses. Among the steady state measurements were conventional stagnation tests at 600 and 800 Wm⁻² respectively. For fitting the dynamic behaviour of the sorption modules an additional 10 dynamic cycle tests of desorption/absorption with varying solar intensity, flows and inlet temperatures were performed. An exemplary result of model calibration is shown in Fig. 5. As can be seen the agreement between experimental and simulated results is very good.

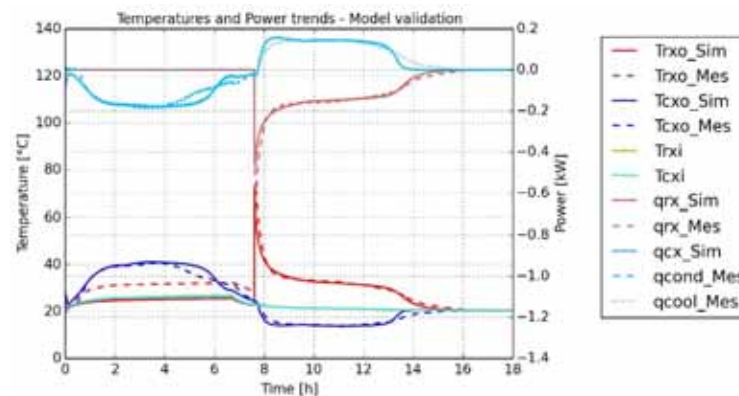


Fig. 5: Fitting of model to dynamic test measurements with 600Wm⁻² intensity and ambient inlet temperatures.

2.5 Control strategy

Control strategies are based on controllers (mainly signal out of hysteresis) combined among them in control schemes: each scheme defines which component has to be turned on or off. The whole control depends on the following variables which can be also easily measured in a real application.

- The indoor temperature: it defines whether the indoor environment needs heating or cooling or if it is in heating or cooling drift conditions.
- The incident direct radiation: it determines whether the solar direct radiation is impinging on the collector plane and therefore whether it is possible to allow desorption, absorption, or heating from the reactor absorber as a standard collector.
- The reactor absorber temperature: it allows controlling the desorption and absorption phases' starts at a sufficient high and low temperature respectively.

- The heat rejection temperature difference and the power distribution temperature difference: these two temperature differences stop cooling or heating distribution when the value is below defined set points.

From these controllers, the following control schemes - referring only to the sorption collectors devices - are generated.

- **Absorption phase** with cooling power generation from the evaporator and heat rejection at the reactor: CE and reactor fans are both started. CE dampers are set in order to take indoor air and distribute the cooled air to the indoor environment. Air flowing through the reactor dampers is taken and rejected from/to the outside. Signal is 1 if there is cooling demand, no direct sunshine on the collector plane, a sufficiently low reactor absorber temperature and if the inlet air is lower than the indoor air.
- **Desorption phase:** solar radiation is absorbed at the reactor and heat has to be rejected at the condenser. Hence, condenser fan starts and outside air is used. Signal is 1 if there is no heating demand, direct sunshine on the collector plane and a sufficiently high reactor absorber temperature.

2.6 Parametric runs and performance indicators

Parametric analyses have been performed changing the climatic location (Stockholm, Stuttgart, Rome) and, the façade orientation (East, South, West), getting sorption collector energy performances and its impacts on the target office room. All other simulation parameters are kept constant through the parametric runs and are calculated from the current prototype measurements as described above.

Simulations results have been compared in terms of standard indicators such as Electric Efficiency Ratio (EER), Solar Fraction (SF), cooling efficiency (η_{cool}), Energy Index (EnIND) and Losses rate (SULOSS), calculated at daily, weekly, monthly and yearly scales with the equation 2, 3, 4 and 5.

$$EER_{cool} = \int \dot{Q}_{SC_{cool}} / \int \dot{Q}_{SC_{electric}} \text{ (eq. 2)}, SF_{cool} = \int \dot{Q}_{SC_{cool}} / \int \dot{Q}_{cool_{dem}} \text{ (eq. 3)},$$

$$\eta_{cool} = \int \dot{Q}_{SC_{cool}} / \int \dot{Q}_{SC_{solar}} \text{ (eq. 4)}, EnIND = \int \dot{Q}_{SC_{cool}} / A_{apcoll} \text{ (eq. 5)}.$$

$\dot{Q}_{SC_{cool}}$ is the sorption collector sensible cooling power calculated as the sensible heat flux removed from the air passing through the collector; $\dot{Q}_{SC_{electric}}$ is the electric power consumption needed for the sorption collector' fans and used to generate cooling (both desorption and absorption phases); $\dot{Q}_{cool_{dem}}$ is the room sensible heating demand; $\dot{Q}_{SC_{solar}}$ is the global solar power available at the collector aperture surface during desorption times and A_{apcoll} is the collector aperture area.

3. Results

Typical operation cycles in cooling mode are shown in Fig. 6. Negative power and energy values indicate cooling. While the direct radiation is impinging the collector plane (roughly from 9 am to 18 pm for a south oriented façade in summer), the reactor absorber reaches the temperature needed to start desorption and the condenser rejects heat at about 40°C to the external environment with a power exchange of about 0.3 kW. Concentration of solute in the CE increases up to almost 1 (minimum cannot be below 0.4). Indoor air temperature is kept within the set point hysteresis thanks to the fancoil. At the point when direct solar radiation is zero and reactor absorber temperature is decreased below 50°C, the cooling generation starts in the CE. Fresh air between 10°C – 15°C is delivered into the room, cooling down the indoor air at a power of about 0.3 kW. In parallel, heat rejection occurs in the reactor with an outlet air temperature peak of about 40°C down to 30°C at the end of the absorption cycle. Absorption lasts for a number of hours depending on the charge rate (up to 7), during which the CE discharges the accumulated power keeping the indoor air between the desired set points. West cases show the less favorable behavior: desorption and therefore absorption start later in the day: cooling loads decrease in the late afternoon when the sorption collector lowers the indoor temperature below the minimum allowed temperature causing a stop in the absorption even if some more cooling power could be still distributed.

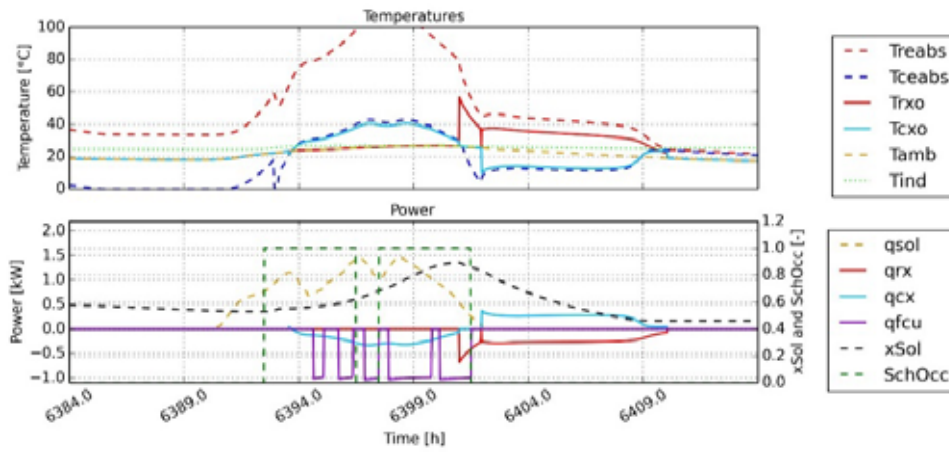


Fig. 6: Late September in Rome for a south oriented façade.

One of the best cases, among the simulated ones, is shown in Fig. 7 in terms of monthly values during the year. For a East oriented façade in Rome, the sorption collector cooling production reaches its maximum value in summer (June) with values of about -50 kWh/m^2 for q_{cool} . η_{cool} trend shows a quite constant value around 20% from February to October. SFcool is above 50% in several months of the mid-season and cold seasons; EERcool is below 10, between 3 and 8 with its maximum in April and its minimum in December.

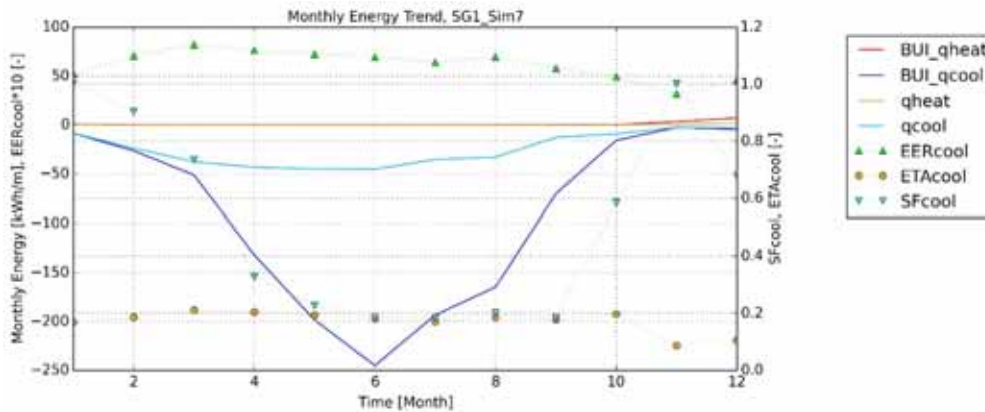


Fig. 7: Yearly trend of monthly values of energy and main performance indicator for east façade orientation in Rome.

Taking Rome as an example, for the three façade integrated sorption collectors, the cooling power delivered to the indoor ambient has two peaks of frequency, one at about -0.2 - 0.3 kW and one close to -0.1 kW (representing the final delivery phase during which the remaining charge is really low). Interesting to be noticed is that South and West are performing better than East in terms of power with about 0.1 kW more in the frequency distribution peaks, even if the latter has a greater number of time step of cooling distribution with power $< 0 \text{ kW}$. South oriented collectors generate the highest cooling powers with values around -0.5 kW .

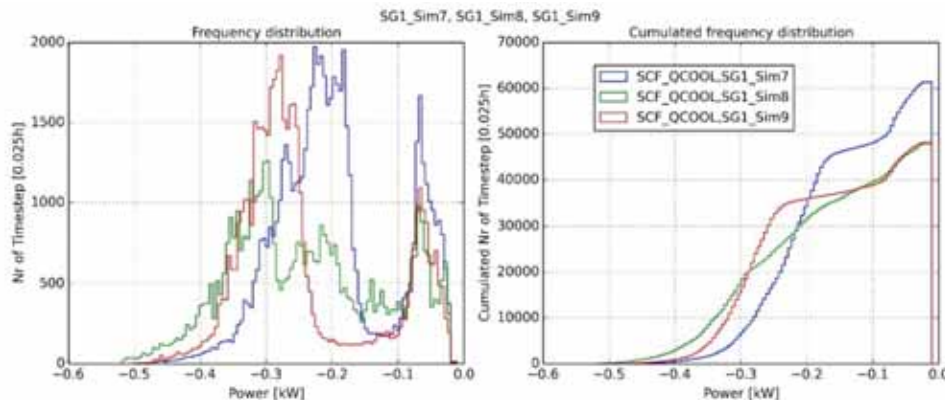


Fig. 8: Frequency and cumulated frequency distribution for the cooling power generated by the sorption collector for the three orientations in Rome. Negative power values indicates cooling.

Tab. 3 reports the yearly performance values for energies and performance indexes for all climates and orientations. SFcool are above 30% for Stockholm, between 23% and 33% in Stuttgart and between 21% and 27% in Rome, with East having always the greater values. EERcool are between 5 and 8 and η_{cool} between 11% and 20%.

Tab. 3: Yearly performances of the façade integrated sorption collector. Negative energy values indicates cooling.

		BUI_qcool	qcool	SFcool	EERcool	η_{cool}	EnIND
		[kWh/y]	[kWh/y]	[%]	[-]	[%]	[kWh/m ² ap/y]
Stockholm	East	-411	-164	40	6.9	19	61.0
	South	-489	-159	32	5.6	11	59.2
	West	-377	-118	31	6.4	14	44.2
Stuttgart	East	-488	-160	33	6.4	20	59.6
	South	-626	-146	23	5.1	11	54.5
	West	-488	-135	28	6.9	16	50.4
Rome	East	-1114	-300	27	6.8	18	112.1
	South	-1330	-285	21	6.0	12	106.4
	West	-1070	-291	27	7.9	20	108.5

4. Discussion

Fig. 6 shows how the cooling distribution from the sorption collector helps in reducing the indoor air temperature (and hence also the energy demand from non-renewable sources). SC cooling can occur during the afternoon, evening and night respectively for East, South and West oriented façades as determined by the control strategy. Values of more than 50% of SFcool for certain months (e.g. East façade in Rome, February and October) can be reached even with only three small collectors; the yearly values are in the range of 30% for East and West façades. Lower performances for south façade in Rome are due to high incidence angles in summer. This solar cooling is yet delivered at too low electrical energy efficiency (EERcool) mainly due to the high pressure drop at the CE (Fig. 7). For a second prototype the heat exchanger will be adapted to lower the pressure drop, which will allow for much higher values of EERcool >10.

Fig. 8 highlights that East oriented façades are the least performing in terms of cooling output power peaks but better performing in terms of energy: hence, besides a good state of charge (good insolation values in the morning), the whole energy stored can be distributed during the room cooling peak loads (midday and afternoon). The lower cooling powers are due to higher heat rejection temperatures during midday and afternoon. West is performing at lower levels in cold climates, improving its performances for hot climate. In fact, West oriented sorption collectors often have remaining charge when the indoor air temperature is already low enough and the cooling delivery has to stop to prevent overcooling. With an optimized control strategy this remaining charge could potentially be used again in the morning and so boost the efficiency slightly.

η_{cool} is calculated dividing the sorption collector output cooling energy by the total solar energy on the sorption collector plane calculated only when desorption occurs. This gives values of η_{cool} coherent with the ones calculated in the tests. It has to be noticed that during absorption the total solar radiation on the façade plane is only diffuse but not negligible. Moreover, optical losses plays an important role in determining η_{cool} due to the presence of the external glazing cover which cut solar radiation contribution for high incidence angles (summer seasons).

5. Conclusions

The integrated sorption façade collector can dramatically simplify thermally driven solar cooling systems by providing a cost effective “plug and play” system solution for the retrofit market without the need for heat rejection units, storages, heat transfer fluid or plumbing. η_{cool} is comparable to simulated and monitored values for roof based systems with the same sorption technology as reported in (Hallström, et al. 2014) and (Blackman, et al. 2014). Solar fractions are high considering the small aperture area available (2.67 m²). The

cooling energy index, however, is significantly lower than roof based systems mainly due to lower insolation on a vertical plane. Yearly electrical efficiencies as well are below the level of the roof top installation because the CE heat exchanger has still to be optimized. Part of the cost increase of the lower cooling energy index can be compensated by the larger center-center distance between the sorption tubes (and hence fewer tubes per unit area), but then sorption tubes of the same length as the roof based concept must be used and not the shorter custom made version manufactured for the current prototype. In general, overall performances are promising and encourage the implementation into real buildings.

Future improvements on the prototype before the demonstration are needed, starting from increasing optical efficiency more than decreasing thermal losses. Letting more solar radiation reaching the absorber surface would lead to better performances in terms of η_{cool} . Pressure drops, especially at the CE heat exchanger, can be improved leading to lower fan electric consumption and therefore to higher values of EERcool. The layout for fans and dampers has to be further assessed in terms of fully decentralized or semi-centralized devices (façade modules in parallel) for the system upscaling. From the modeling point of view, heat pump heating mode, latent cooling and more detailed building physics calculations will be implemented (sorption collector and DSF interaction, indoor comfort evaluation, air patterns impacts). Control strategies and main driving parameters (e.g. mass flow rates) optimization could give useful inputs for further improvements of the operation phase. A cost-benefit analysis is needed to assess the technology impact on office building retrofit market.

The façade solar cooling system has an interesting potential also for providing additional free cooling and air renovation in combination with active heating/cooling. This is possible during absorption by opening the dampers with a phase shift so that cooler outdoor air is further cooled in the CE and blown into the room, while extracting warmer indoor air to the outside through the reactor as means for heat rejection. This would of course only make sense during times when outdoor temperatures are lower than indoor temperatures or when fresh air is needed. The potential could quite easily be determined through simulation.

6. Acknowledgement

The research leading to these results has received funding from the European Union's Seventh Programme for research, technological development and demonstration under grant agreement No. 314461 –iNSPiRe. The European Union is not liable for any use that may be made of the information contained in this document which is merely representing the authors view. Moreover, the authors wish to express their gratitude to Swedish Research Council Formas for the financial support to the research leading to the results presented and to the many employees of ClimateWell AB, Fraunhofer ISE and Eurac collaborating in these projects.

7. Nomenclature

Quantity	Symbol
Sorption Collector Façade integrated	SCF
Sorption Collector	SC
Reactor	RE
Condenser/Evaporator	CE
Simulated	_Sim
Measured	_Mes

Quantity	Symbol	Unit
Reactor absorber temperature	Treabs	°C
Condenser/evaporator absorber temperature	Tceabs	°C
Reactor outlet air temperature	Trxo	°C
Condenser/evaporator outlet air temperature	Texo	°C
Indoor ambient temperature	Tind	°C
Outdoor ambient temperature	Tamb	°C

Heat and heat flux exchanged across the reactor	Qrx, qrx	kWh, kW
Heat and heat flux exchanged across the reactor	Qcx, qcx	kWh, kW
Global solar energy and power radiation on the collector aperture surface	Qsol, qsol	kWh, kW
Power supplied from the fancoil to indoor air	qfcu	kW
Cooling energy index	EnINDcool	kWh/m ²
Room cooling demand	BUI_qcool	kWh/y
Sorption collector cooling energy production	qcool	kWh/y
Sorption collector heating energy production	qheat	kWh/y
Electric Efficiency Ratio in cooling	EERcool	-
Solar Fraction of cooling	SFcool	-
Solar thermal efficiency (total cooling / total insolation)	Etacool	-
Average mass fraction of solute in reactor	xSol	-
Schedule of worker presence in the office	SchOcc	-
Glazing thermal transmittance	U-value	W/m ² K
Glazing solar energy transmittance	g-value	-
Glazing transmittance, absorptance and reflectance	τ, α, ρ	-

8. References

- Hallström, O., Földner, G., Spahn H.J., Schnabel L., Salg F., 2014. Development of Collector Integrated Sorption Modules for Solar Heating and Cooling: Performance Simulation. *Energy Procedia* 48 (2014) 67-76.
- Blackman, C., Hallström, O., Bales, C., 2014. Demonstration of solar heating and cooling system using sorption integrated solar thermal collectors, *Conference Proceedings Eurosun 2014*, 16-19 September. Aix-les-Bains (France).
- Itard, L., Meijer, F., Vrins, E., Hoiting H., 2008. *Building Renovation and Modernisation in Europe : State of the art review*, ERABUILD project.
- Földner, G., Schnabel, L., Horn, P., Spahn, H. J., Schmidt, C., Thoma, C., Salg, F., Schossig, P., 2013. KollSorp – Entwicklung eines kollektorintegrierten Sorptionssystems zur solaren Kühlung und Heizungsunterstützung. 23. Symposium Thermische Solarenergie, OTTI. Bad Staffelstein (Germany).
- Di Pasquale, C., Fedrizzi, R., Bellini, A., D'Antoni, M., Bales, C., Gustafsson, M., Ochs, F., Dermentzis, G., Birchall, S., August 2014. D2.1c Simulation Results of Reference Buildings, Inspire EU FP7 project, www.inspirefp7.eu (1.9.2014)
- Haller, M., 2012. TRNSYS Type 832 v5.00 Dynamic Collector Model by Bengt Perers, Updated Input-Output Reference, Hochschule für technik Rapperswil, SPF Institut für Solartechnik.